

Oncolytic herpes virus armed with vasculostatin in combination with bevacizumab abrogate glioma invasion via the CCN1 and AKT signaling pathways

Running title: Oncolytic herpes virus and bevacizumab combination

Yusuke Tomita ¹, Kazuhiko Kurozumi ¹, Ji Young Yoo ², Kentaro Fujii ¹, Tomotsugu Ichikawa ¹, Yuji Matsumoto ¹, Atsuhito Uneda¹, Yasuhiko Hattori¹, Toshihiko Shimizu ¹, Yoshihiro Otani ², Tetsuo Oka ¹, Balveen Kaur ², Isao Date ¹

¹Department of Neurological Surgery, Okayama University Graduate School of Medicine, Dentistry and Pharmaceutical Sciences, Okayama, Japan

²Department of Neurosurgery, University of Texas Health Science Center at Houston, Houston, Texas, USA

Correspondence should be addressed to Kazuhiko Kurozumi:

Department of Neurological Surgery, Okayama University Graduate School of Medicine, 2-5-1 Shikata-cho, Kita-ku, Okayama 700-0914, Japan

Tel: (+81) 86-235-7336

Fax: (+81) 86-227-0191

E-mail: kkuro@md.okayama-u.ac.jp

Total number of figures: 6 figures and 4 supplementary figures

Funding

This study was supported by Japan Society for the Promotion of Science to K.Kurozumi (No. 26462182; No.17K10865).

Conflict of Interest

All authors certify that they have no affiliations with, or involvement in, any

organization or entity with any financial interest (such as honoraria; educational grants; participation in speakers' bureaus; membership, employment, consultancies, stock ownership, or other equity interest; and expert testimony or patent-licensing arrangements) or non-financial interest (such as personal or professional relationships, affiliations, knowledge, or beliefs) in the subject matter or materials discussed in this manuscript.

Abbreviations

HSV, herpes simplex virus; OV, oncolytic virus; HSVQ, attenuated herpes simplex virus; RAMBO, Rapid Antiangiogenesis Mediated By Oncolytic virus; rQNestin34.5, oncolytic HSV-1 mutant expressing ICP34.5 under nestin promotor; 34.5ENVE, viral ICP34.5 Expressed by Nestin promotor and Vstat120 Expressing; VEGF, vascular endothelial growth factor; BEV, bevacizumab; CM, conditioned medium; CSK, C-terminal Src kinase; SHC3, SHC (Src homology 2 domain containing) transforming protein 3; PTK2, protein tyrosine kinase 2; CAV, caveolin 3; SOS1, Son of sevenless homolog 1 (Drosophila); CCN1, cysteine-rich protein 61; GAPDH, glyceraldehyde 3-phosphate dehydrogenase

Keywords: glioma, invasion, bevacizumab, VEGF, oncolytic herpes virus

Abstract

Anti-vascular endothelial growth factor treatments such as bevacizumab have demonstrated convincing therapeutic advantage in glioblastoma patients. However, bevacizumab has also been reported to induce invasiveness of glioma. In this study, we examined the effects of Rapid Antiangiogenesis Mediated By Oncolytic virus (RAMBO), an oncolytic herpes simplex virus-1 expressing vasculostatin, on bevacizumab-induced glioma invasion. The effect of the combination of RAMBO and bevacizumab *in vitro* was assessed by cytotoxicity, migration, and invasion assays. For *in vivo* experiments, glioma cells were stereotactically inoculated into the brain of mice. RAMBO was intratumorally injected seven days after tumor inoculation, and bevacizumab was administered intraperitoneally twice a week. RAMBO significantly decreased both the migration and invasion of glioma cells treated with bevacizumab. In mice treated with bevacizumab and RAMBO combination, the survival time was significantly longer and the depth of tumor invasion was significantly smaller than those treated with monotherapy of bevacizumab. Interestingly, RAMBO decreased the expression of cysteine-rich protein 61 and phosphorylation of AKT, which were increased by bevacizumab. These results suggest that RAMBO suppresses bevacizumab-induced glioma invasion, which could be a promising approach to glioma therapy.

Introduction

Gliomas represent about 30% of primary brain tumors. Despite numerous efforts to develop new treatments for malignant gliomas, therapeutic options remain limited and the prognosis is still poor (1,2). Temozolomide is the only agent validated for its effectiveness on overall survival, and its concomitant use with radiotherapy is the standard therapy for malignant glioma (3). Many investigators continue to seek novel therapeutic approaches for glioma including surgery, chemotherapy, radiotherapy, immunotherapy, and combination therapies.

Antiangiogenic therapy is one of the strategies used to treat glioblastoma. Glioblastoma cells secrete high levels of vascular endothelial growth factor (VEGF). Bevacizumab binds to all VEGF isoforms, causing reduced tumor vascularization, reduced vascular permeability, and the inhibition of tumor growth (4). Bevacizumab, which targets pro-angiogenic VEGF, is a recombinant humanized monoclonal antibody that was approved as a chemotherapeutic agent for primary and recurrent glioblastoma in Japan. Its clinical use is increasing, even though its advantages on overall survival were lacking in previous trials (5,6). Recent studies indicated that anti-VEGF therapy induced glioma invasion via several mechanisms including the integrin-related pathway (7,8), indicating it is important to test the potential uses of bevacizumab in combination therapies.

Oncolytic viral (OV) therapy has appeared as a promising treatment modality that utilizes the tumor-specific properties (9). Oncolytic herpes simplex viruses (HSVs) is designed to replicate and have cytotoxicity selectively in tumor cells, but not in normal tissues. Oncolytic HSVs include genetically engineered viruses such as talimogene laherparepvec, and a spontaneously mutated virus without the insertion of foreign genes, such as HF10 (10). Intralesional talimogene laherparepvec administration improved durable response rates in a randomized phase III trial (11), for which the accelerated Food and Drug Administration approved to use oncolytic HSVs for patients with recurrent melanoma. Phase I and II trials of HF10 in patients with recurrent metastatic breast carcinoma, recurrent head and neck squamous cell carcinoma, advanced pancreatic carcinoma, refractory and superficial cancers, and melanoma have been successfully conducted (10). There are several challenges regarding oncolytic HSVs, such as their rapid clearance by host immune responses, and limited intratumoral spread of the virus. To overcome these challenges, genetic engineering of OVs or combination therapy with OVs and systemic treatments such as molecular targeting drugs have been suggested (12-17).

Vasculostatin (Vstat120), the extracellular fragment of brain-specific angiogenesis inhibitor 1 (BAI-1), is a potent anti-angiogenic and anti-tumorigenic factor (18,19). Vasculostatin contains an integrin-antagonizing RGD (Arg-Gly-Asp) motif, five thrombospondin type 1 repeats, a GPS (G-protein-coupled receptor proteolytic site) domain and seven-transmembrane domains (18,20). The BAI-1 expression is negatively correlated with pathological grading, angiogenesis and brain edema in gliomas (21). A vasculostatin-armed oncolytic HSV-1, termed Rapid Antiangiogenesis Mediated By Oncolytic virus (RAMBO) , significantly suppressed intracranial and subcutaneous glioma growth in

mouse glioma models compared with control virus (12,13). Furthermore, Fujii et al. reported the efficacy of combination therapy with cyclic RGD peptide and RAMBO for malignant glioma (12). We hypothesized that bevacizumab and RAMBO combination therapy has a synergic effect, because vasculostatin expressed by RAMBO might antagonize integrin-related pathways induced by bevacizumab.

In this study, we evaluated RAMBO and bevacizumab combination treatment of glioma. RAMBO reduced bevacizumab-induced glioma invasion with vasculostatin expressed by RAMBO-infected glioma cells. Evaluation of the invasive mechanism revealed the decreased activation of AKT signaling pathways in cells treated with combined RAMBO and bevacizumab.

Materials and Methods

Cell lines, drugs, and viruses

U87ΔEGFR was initially engineered by the Cavenee laboratory at the Ludwig Institute for Cancer Research, New York, NY, USA. U251MG was obtained from Dr. Balveen Kaur at Ohio State University, Columbus, OH, USA. U87MG was obtained from the American Type Culture Collection. Vero cells were purchased from American Type Culture Collection and used for viral replication. Glioma cells and Vero cells were prepared and maintained as described previously (14). MGG23 was provided by Dr. Hiroaki Wakimoto and cultured as previously described (22,23). All cells were cultured at 37°C in an atmosphere containing 5% CO₂. U87ΔEGFR, U251MG, and U87MG were authenticated by Promega (Madison, WI, USA) via short tandem repeat profiling in December 2016. Mycoplasma was negative in all cells.

Bevacizumab was purchased from Genentech (San Francisco, CA)/Roche (Basel, Switzerland)/Chugai Pharmaceutical Co (Tokyo, Japan).

The construction and efficacy of HSVQ, a first generation OV deleted for both copies of ICP34.5 and disrupted for ICP6, and RAMBO, a Vstat120-expressing OV within the context of HSVQ1, have been previously described (13,14,17,24,25). HSVQ1 was engineered by the Chiocca laboratory, and RAMBO was originally engineered by the Chiocca and Kaur laboratories.

Cytotoxicity assay

The cytotoxicity of U87ΔEGFR, U251MG, U87MG, and MGG23 glioma cells were analyzed using the water-soluble tetrazolium (WST)-1 according to the manufacturer's instructions (Roche Molecular Biochemicals, Mannheim, Germany). We performed WST-1 quantitative colorimetric assay for cell survival as previously described (12).

In vitro migration assay

U87ΔEGFR, U251MG, and U87MG glioma cells were infected with RAMBO or HSVQ dissolved in

DMEM with 0.1% FBS at MOI 2, and conditioned medium (CM) was harvested 14 hours later by centrifugation, as previously reported (12).

The scratch wound assay was performed as previously described (12,26). Glioma cells were exposed to bevacizumab from 72 hours before assessment. Medium was changed to CM or DMEM with 0.1% fetal bovine serum, and the indicated concentration of bevacizumab was added. Glioma cells were assessed by counting migrating cells in the area of the gap every 6 hours to 24 hours (Keyence, Osaka, Japan).

An *in vitro* migration assay was performed using a 24-well plate and ThinCert™ (8 µm-pore, 24-well format, Greiner Bio-One) according to the manufacturer's instructions, as previously reported (26,27).

In vitro invasion assay

The *in vitro* invasion assay was performed using a BioCoat Matrigel invasion chamber (24-well format, Corning Incorporated) according to the manufacturer's instructions. 5×10^4 cells were seeded in CM or DMEM with 0.1% FBS in the upper chamber, followed by treatment with bevacizumab or PBS, as previously described (26,27).

In another *in vitro* invasion assay, MGG23 cells were seeded in a 96-well ultra-low attachment plate (Costar, Corning Incorporated, NY, USA) at a density of 1.0×10^3 cells/well in 25 µl of medium, followed by treatment with viruses and bevacizumab to the indicated wells. After centrifugation to assemble all the cells to the center, matrigel (25 µg/insert, Becton Dickinson, Franklin Lakes, USA) was added to each well. Digital photomicrographs of the midplane of spheroids were taken daily with a BZ-8100 microscope (Keyence, Osaka, Japan). Core and invasive diameter were measured using ImageJ (<http://rsb.info.nih.gov/ij/>) and the radius of invasion was calculated, as previously described (28).

Brain Xenografts

All experiments were conducted in accordance with the guidelines of the Okayama University Animal Research Committee. All procedures and animal protocols were approved by the Committee on the Ethics of Animal Experimentation at Okayama University, as previously described (27). U87ΔEGFR cells were injected into athymic mice (CLEA Japan Inc., Tokyo, Japan), and MGG23 cells were injected into severe combined immunodeficiency mice (Charles River Laboratories Japan, Yokohama, Japan), respectively. Glioma cells (2×10^5 cells) were stereotactically injected into the right frontal lobe, as previously described (7). Five days after implantation of the glioma cells, mice were treated with bevacizumab at the indicated concentration or PBS intraperitoneally twice a week. Seven days after inoculation of the glioma cells, anesthetized mice were stereotactically injected with the indicated plaque forming units of RAMBO at the same location as the tumor.

In both mouse glioma models, the survival time was assessed with a Kaplan-Meier survival analysis. U87ΔEGFR harboring mice were sacrificed 18 days after tumor implantation or if they showed signs of

morbidity for pathological analysis, qRT-PCR and western blotting. MGG23 harboring mice were sacrificed 50 days after tumor implantation for pathological analysis.

Immunohistochemistry

Surgically excised brains from mouse glioma models were fixed with 4% paraformaldehyde, embedded in paraffin, and 4- μ m sections were prepared. Immunohistochemistry analyses were carried out as previously described (7,25). Anti-human leukocyte antigen monoclonal antibody (1:100 dilution, Abcam Inc.) was used for the staining, and mouse immunoglobulin was used as a negative control. The sections were stained with Dako Envision + System-HRP Kit in accordance with the manufacturer's protocol (DakoCytomation), and were counterstained with hematoxylin. Immunohistochemistry samples were observed with a BZ-8100 microscope.

RNA isolation, cDNA synthesis and qRT-PCR

We isolated total RNA from the cell lines or tumor specimens. Syntheses of cDNA and qRT-PCR procedures were conducted as previously described (26,29). As an internal control, we used glyceraldehyde 3-phosphate dehydrogenase (GAPDH) mRNA. The primer sequences used were as follows: Human C-terminal Src kinase (CSK) primers: forward, gacgtgtggagtttcggaat; reverse, agctgctctcggagctgtag. Human SHC (Src homology 2 domain containing) transforming protein 3 (SHC3) primers: forward, agagtgtggaaggctcagga; reverse, gtgcttttcagcgagaacc. Human protein tyrosine kinase 2 (PTK) primers: forward, ctctgcagttccccagag; reverse, ccagtggttggtcactat. Human Caveolin 3 (CAV) primers: forward, ttgccaagaggcagctact; reverse, accctttactggagccacct. Human Son of sevenless homolog 1 (SOS1) primers: forward, ccttgcttgaggtttctgc; reverse, gcagatgctgatgaaccaga. Human cysteine rich protein 61 (CCN1) primers: forward, cctcgcactctatacaacccttta; reverse, gattctgacactcttctccctgt. Human GAPDH primers: forward, gacctgccgtctagaaaaacc; reverse, gctgtagccaaattcgtgtc.

Western blot analysis

We prepared cell lysates and proteins using RIPA buffer and phenyl-methylsulfonyl fluoride (Cell Signaling Technology, Danvers, MA, USA), as previously described (28). Then, we performed western blotting as previously described (15,27). After blocking, membranes were incubated overnight with primary antibodies (anti-CYR61, 1:100, Novus Biologicals, Littleton, Co., USA; anti-AKT, 1:1000, Cell Signaling Technology; anti-p-AKT, 1:1000, Cell Signaling Technology; and anti-GAPDH, 1:1000, Cell Signaling Technology; anti-BAI1, 1:200, WuXi Biosciences) at 4°C. The secondary antibodies used were horseradish peroxidase-conjugated anti-mouse IgG and HRP-conjugated anti-rabbit IgG (Cell Signaling Technology, 1:5000). HRP signals were analyzed by the VersaDoc molecular imaging system (Bio-Rad, Hercules, CA, USA).

Statistical analysis

The changes in cell death, migration and invasion were analyzed using one-way analysis of variance (ANOVA) followed by Tukey's post hoc test. Kaplan-Meier survival curves were compared using the log-rank test. Data on mRNA expression obtained by quantitative real-time PCR were analyzed by one-way ANOVA followed by Scheffe's post hoc test. Data on protein expression obtained by western blotting were analyzed using ANOVA followed by Tukey's post hoc test. All statistical analyses were performed using SPSS statistical software (version 20; SPSS, Inc., Chicago, IL, USA).

Results

Cytotoxic effect of combination therapy with bevacizumab and RAMBO

The cytotoxic effect of combined bevacizumab and RAMBO on glioma cells was investigated by WST-1 proliferation assay. Glioma cell lines and glioma stem cells were incubated with the indicated concentrations of bevacizumab or RAMBO at the indicated MOI. Treatment with RAMBO decreased viable cells compared with saline as a control in a time-dependent manner. After treatment with RAMBO, U87ΔEGFR cells were aggregated and floated from the dishes, whereas MGG23 cells were dissociated and adhered to the dishes (Figure 1A). There was a significant decrease in viable cells treated with RAMBO compared with saline treatment of each cell line at 48 and 72 hours (U87ΔEGFR, $p < 0.001$; U251MG, $p < 0.001$; U87MG, $p < 0.001$; MGG23, $p < 0.001$). However, bevacizumab had no cytotoxic effect against glioma cells and did not increase the cytotoxicity of RAMBO against glioma cells (Figure 1B).

Supernatant from RAMBO-infected glioma cells inhibits glioma cell migration in vitro.

To examine the *in vitro* effect of vasculostatin on GBM cell migration over time, we performed a scratch wound assay using bevacizumab and conditioned medium (CM). The supernatant of malignant glioma cells infected by RAMBO was centrifuged and filtrated to eliminate virus and cell lysates, then it was used as RAMBO-CM. Infection of each cell line by oncolytic virus was detected by the expression of GFP implanted into the viral sequence (Supplementary Figure 1A). In the RAMBO-infected glioma cells, the expression of vasculostatin was detected by western blotting (Supplementary Figure 1B). Vasculostatin in CM had no cytotoxic effect against glioma cells similar to fresh medium (Supplementary Figure 1C). The rate of migrating cells was assessed every 6 hours after scratch formation and we performed Giemsa staining 24 hours after scratch formation (Figure 2A, Supplementary Figure 2A-B). RAMBO CM significantly reduced the rate of migration of each cell line compared with saline control (U87ΔEGFR: $p < 0.001$, U251MG: $p < 0.001$, and U87MG: $p < 0.001$). Furthermore, the rate of migrating cells induced by bevacizumab treatment was reduced by RAMBO CM (U87ΔEGFR: $p < 0.001$, U251MG: $p < 0.001$, and U87MG: $p < 0.001$) (Figure 2B). We also performed another migration assay using ThinCert

for an enhanced quantitative analysis (Figure 2C). Bevacizumab significantly increased the migration of each cell line compared with saline control (U87ΔEGFR: $p<0.001$, U251MG: $p<0.001$, and U87MG: $p<0.001$). Furthermore, the rate of migrating cells induced by bevacizumab treatment was reduced by RAMBO CM (U87ΔEGFR: $p<0.001$, U251MG: $p<0.001$, and U87MG: $p=0.010$) (Figure 2D).

RAMBO-infected glioma cells inhibit glioma cell invasion in vitro.

To examine the *in vitro* effect of vasculostatin on GBM cell invasion, we performed a matrigel invasion assay with a Corning chamber using bevacizumab and CM. The supernatant of malignant glioma cells infected by RAMBO or HSVQ was centrifuged and filtrated to eliminate virus and cell lysate, then they were used as RAMBO-CM or HSVQ-CM. The expression of vasculostatin was detected by western blotting in RAMBO-infected glioma cells but not in HSVQ-infected glioma cells (Supplementary Figure 1B). Giemsa staining was performed 24 hours after seeding glioma cells into the upper chamber, and then cells invading through the membrane were counted (Figure 3A). RAMBO CM significantly reduced the number of invading cells of each cell line compared with saline control (U87ΔEGFR: $p<0.001$, U251MG: $p<0.001$, and U87MG: $p<0.001$). Furthermore, the invading cells induced by bevacizumab treatment were reduced by RAMBO CM (U87ΔEGFR: $p<0.001$, U251MG: $p<0.001$, and U87MG: $p<0.001$) (Figure 3B).

To examine the *in vitro* effect of vasculostatin on GBM stem cell invasion, we performed Matrigel invasion assays ($p<0.01$) (Figure 3C). After measurement of the core and invasive diameter, the proportion of invasion was calculated. Bevacizumab significantly increased the proportion of glioma cell invasion compared with saline controls ($p=0.001$). Combination therapy with bevacizumab and RAMBO significantly inhibited bevacizumab-induced glioma cell invasion of MGG23 cells ($p=0.001$), whereas combination therapy with bevacizumab and HSVQ did not inhibit bevacizumab-induced glioma cell invasion of MGG23 ($p=0.062$) (Figure 3D).

Anti-tumor efficacy of combination therapy with bevacizumab and RAMBO in xenograft mice.

The antitumor effect of combination with bevacizumab and RAMBO was tested in mice harboring intracerebral U87ΔEGFR glioma cells (Figure 4A). The survival of mice in each group (7 mice per group) was compared by Kaplan-Meier analysis.

Control mice treated with PBS had a median survival of 17 days after tumor cell implantation, and mice treated with RAMBO had a median survival of 28 days that was similar to that of PBS-treated mice. Mice treated with bevacizumab had a median survival of 37 days. Mice treated with HSVQ and bevacizumab combination had a median survival of 46 days, which did not reach statistical significance compared with bevacizumab monotherapy ($p=0.075$). However, mice treated with bevacizumab and RAMBO combination had a median survival of 64 days, which was significantly longer than mice treated

with PBS, RAMBO alone, bevacizumab alone, and bevacizumab and HSVQ combination (Log-rank test: $p < 0.001$, $p < 0.001$, $p < 0.001$, and $p = 0.001$, respectively) (Figure 4B).

Next, we performed survival analysis using glioma stem cells. We compared immunodeficient mice bearing MGG23 cells treated with saline, bevacizumab at 10 mg/kg, HSVQ at 1.0×10^5 pfu as monotherapy, HSVQ at 1.0×10^5 pfu and bevacizumab at 10 mg/kg, and RAMBO at 1.0×10^5 pfu and bevacizumab at 10 mg/kg. Control mice treated with PBS had a median survival of 62 days, and mice treated with bevacizumab had a median survival of 61 days. Mice treated with RAMBO as monotherapy had a median survival of 65 days, which was significantly longer than mice treated with PBS ($p = 0.001$). Mice treated with HSVQ and bevacizumab combination had a median survival of 65 days, which reached statistical significance compared with bevacizumab monotherapy ($p = 0.001$). Furthermore, mice treated with bevacizumab and RAMBO combination had a median survival of 70 days, which was significantly longer than mice treated with bevacizumab monotherapy, RAMBO monotherapy, HSVQ and bevacizumab combination, or untreated mice ($p = 0.001$, $p = 0.005$, $p = 0.001$, and $p = 0.001$, respectively) (Figure 5A).

Effect of RAMBO on bevacizumab-induced invasion in vivo.

To address the therapeutic effect against glioma invasion, we evaluated combination therapy with RAMBO at 1.0×10^5 pfu and bevacizumab at 10 mg/kg. RAMBO and bevacizumab were administered using the same schedule as for the survival analysis (Figure 4A).

Immunohistochemical staining using anti-human leukocyte antigen was performed, and then glioma invasion was assessed (Figure 4C). After treatment with bevacizumab, the tumor border showed tumor invasion. Anti-VEGF therapy with bevacizumab significantly increased cell invasion compared with saline controls ($p = 0.010$). However, combination therapy with bevacizumab and RAMBO significantly decreased the depth of glioma invasion induced by bevacizumab ($p = 0.006$, Figure 4D).

Next, immunodeficient mice harboring MGG23 glioma stem cells were sacrificed at 50 days after tumor implantation, and immunohistochemical staining with anti-human leukocyte antigen was performed. MGG23 cells treated with bevacizumab as monotherapy showed a greater invasion to the ipsilateral cerebral cortex adjacent to the injection site and to the contralateral corpus callosum compared with saline controls or the bevacizumab and RAMBO treated group (Figure 5B). Invasion activity was assessed, as previously reported (27). There was a significant increase of glioma cells invading into the cerebral cortex in the MGG23 cell treated with bevacizumab group compared with saline controls (ipsilateral cortex: $p = 0.016$, contralateral cortex: $p < 0.001$). However, combination therapy with bevacizumab and RAMBO significantly decreased the depth of glioma invasion induced by bevacizumab (ipsilateral cortex: $p = 0.002$, contralateral cortex: $p < 0.001$, Figure 5C). These results indicated that RAMBO reduced invasion with bevacizumab.

Mechanism of combination therapy in the U87ΔEGFR orthotopic mouse model

To investigate the mechanism of the anti-tumor effect of combination therapy with bevacizumab and RAMBO, we performed quantitative PCR analysis. We chose the integrin-related cell adhesion pathway and hepatocyte growth factor receptor signaling pathway because we previously reported its relationship to bevacizumab-induced invasion (7). Relative expression levels of CSK, SHC3, PTK, CAV, SOS1 and CCN1 in the U87ΔEGFR mouse model with bevacizumab were upregulated 1.84-, 1.35-, 2.35-, 6.98-, 3.95- and 3.34-fold, respectively compared with the control group. In particular, only CCN1 expression was significantly reduced in tumors treated with bevacizumab and RAMBO as combination therapy compared with those treated with bevacizumab alone (Figure 6A-6F, $p < 0.05$).

Western blotting was performed to investigate the relationship between CCN1 and the AKT pathway (Figure 6G). Tumors treated with bevacizumab showed significantly higher CCN1 activation than those treated with saline ($p = 0.013$) and those treated with bevacizumab and RAMBO as combination therapy ($p = 0.001$). In addition, tumors treated with bevacizumab showed significantly higher p-AKT at Ser473 than those treated with saline ($p = 0.024$), but bevacizumab and RAMBO as combination therapy significantly reduced AKT phosphorylation compared with bevacizumab ($p < 0.001$, Figure 6H). Full scans of the western blotting are shown in Supplementary Figure 3.

These results demonstrated that vasculostatin expressed by RAMBO and ENVE34.5 reduced CCN1 expression and AKT phosphorylation induced by bevacizumab.

Discussion

Our data showed that U87ΔEGFR-bearing mice treated with bevacizumab had significantly longer survival than those treated with saline. Although U87dEGFR has a poor-invasive phenotype in contrast to clinical glioblastomas, this cell line has been used in several experimental studies to evaluate glioma invasion. In contrast to U87ΔEGFR, bevacizumab had no significant anti-tumor effect against MGG23-bearing mice compared with saline, which was similar to the results of multiple Phase III clinical trials. A study using a mouse model reported showed that bevacizumab significantly reduced tumor growth (30). Our results showed that invasive activity increased by bevacizumab seemed to counteract the effectiveness of bevacizumab in the diffuse invasion glioma model. Moreover, our experiments using two different mouse glioma models indicated that RAMBO inhibited glioma cell invasion induced by bevacizumab, resulting in a synergistic effect.

Previous reports indicated that tumor invasiveness was increased by anti-VEGF therapy (7). de Groot et al. described three patients who, during bevacizumab therapy, developed infiltrative lesions visible by MRI and reported pair imaging features seen on MRI with histopathologic findings (31). In this report, we showed that glioma migration and invasion were increased by bevacizumab, similar to previous reports (7,32). Interestingly, our data also showed that invasive activities of glioma cells were increased by bevacizumab both in the poor-invasive model using U87ΔEGFR and in the diffuse invasive model

using MGG23, indicating that bevacizumab increased glioma cell invasion regardless of the original invasive activity.

RAMBO is composed of cDNA encoding for human vasculostatin (Vstat120) within the backbone of HSVQ (13). Vasculostatin was reported to enhance the anti-tumor effect of oncolytic HSV-1 (13,33). Vasculostatin is an extracellular fragment of brain angiogenesis inhibitor 1, whose expression is reduced in several malignancies (20,24,34-36). The re-expression of vasculostatin had an anti-angiogenic effect, which enhanced antitumor therapeutic efficacy (9,37). Vasculostatin was expressed only from RAMBO-infected glioma cells, which indicated that the effect of vasculostatin was only seen in cells or mice treated with RAMBO. Interestingly, combination therapy with RAMBO and bevacizumab but not HSVQ reduced bevacizumab-induced migration and invasion, and prolonged the survival time of glioma-bearing mice compared with combination therapy with HSVQ and bevacizumab. These results indicated that vasculostatin increases anti-tumor effects by reducing glioma migration and invasion.

The integrin-related cell adhesion pathways were reported to be involved in the mechanism of glioma invasion. DeLay et al. revealed a hyperinvasive phenotype, a resistance pattern of glioblastoma, after bevacizumab therapy and which was upregulated with integrin $\alpha 5$ and fibronectin 1 (38). Jahangiri et al. showed that c-Met and $\beta 1$ integrin were upregulated in bevacizumab-resistant glioblastomas (32). We previously reported that bevacizumab treatment led to increased cell invasion via an integrin signaling pathway (7).

Oncolytic HSV-1 therapy increases integrin-activating CCN1 protein in the tumor extracellular matrix. Kurozumi et al. reported that the oncolytic HSV-1 infection of tumors induced angiogenesis and upregulated CCN1 (9). Haseley et al. reported that CCN1 limited the efficacy of oncolytic viral therapy via an integrin signaling pathway that mediated activation of a type-I antiviral interferon response (39). RAMBO contains vasculostatin in its construct and has five thrombospondin type 1 domains within its N terminal sequence and an integrin antagonizing RGD motif (13,17,19,40,41). Here, we report that CCN1 expression was upregulated by bevacizumab, and that its upregulation was suppressed by RAMBO. Previous reports showed that HSV-1 without vasculostatin increased CCN1 expression in glioma cells (9). Our results showed that HSV-1 expressing vasculostatin decreased CCN1 expression, indicating that the expression of vasculostatin by oncolytic HSV reduced CCN1 induction by HSV-1 itself and by bevacizumab.

The relationship between CCN1 and the AKT pathway was evaluated previously. In tumor cells, high CCN1 expression was related to high Akt phosphorylation (42). Several reports indicated that targeting CCN1 expression might mediate AKT phosphorylation and tumor cell migration(43,44). From our data, combination therapy with bevacizumab and RAMBO significantly decreased the phosphorylation of AKT. Paw et al. previously reported a relationship between the PI3K/AKT pathway and MMP9 expression, which induced glioma cell invasion (45). Therefore, glioma cell invasion via the CCN1/Akt pathway was reduced by vasculostatin expressing oncolytic virus but induced by bevacizumab.

The efficacy of combination viral therapy and chemotherapy has been reported previously. Cyclic RGD peptide had a synergistic effect with viral therapy including adenovirus and HSV-1 (12,16). Ikeda et al. showed that cyclophosphamide substantially increased herpes viral survival and propagation, leading to neoplastic regression (46). Regarding anti-VEGF therapy, several reports described enhanced viral distribution in tumors (30,47). In our study, the mechanism of the synergistic effect observed with bevacizumab and RAMBO involved the bevacizumab-enhanced distribution of RAMBO in the tumors, and RAMBO-induced reduction of glioma cell invasion promoted by bevacizumab.

CCN1 interacts with integrins, such as $\alpha\beta3$, $\alpha6\beta1$, $\alpha\beta5$, and $\alpha11\beta3$, leading to a wide range of biological activities, including cell adhesion, migration, and invasion (48). In addition, exogenous CCN1 in the glioma ECM orchestrated a cellular antiviral response that reduced viral replication and limited the efficacy of the oncolytic virus (39). In this paper, we showed the synergistic effect of combined bevacizumab and RAMBO combination against glioma cells. This synergetic effect might not be clinically relevant because we only used cell lines without heterogeneity, although our survival analysis indicated bevacizumab and RAMBO combination therapy was effective even against a diffuse invading model using glioma stem cells. In the future, we plan to evaluate the effectiveness of bevacizumab or RAMBO combinations using several types of glioma stem cells or primary cultures from glioblastoma patients, that will be more relevant to clinical trials.

Bevacizumab monotherapy or combination treatment with radiation and/or temozolomide is well tolerated and exhibits modest antitumor activity (6,49). Although bevacizumab has not been shown to extend overall survival, it may have additional benefits in the setting of immunotherapy (50). Recently, Currier et al. reported that the combined effect of oncolytic HSV virotherapy and anti-VEGF antibodies was in part due to the modulation of a host inflammatory reaction to virus (51). In addition, Oka et al. reported that CD8- and CD11c-positive cells infiltrated tumors treated with adenovirus vector (15). We intend to evaluate the other combination therapies of bevacizumab and other oncolytic viruses, molecular targeted therapy, and immunotherapy.

Our results indicate that combination therapy with bevacizumab and RAMBO had additional therapeutic effects compared with monotherapy using bevacizumab or oncolytic virus. RAMBO-infected glioma cells significantly reduced glioma migration and invasion induced by bevacizumab both *in vitro* and *in vivo*. Combination therapy with bevacizumab and RAMBO significantly increased the anti-tumor effect in a mouse glioma model. CCN1 expression was modulated by RAMBO to activate or inhibit AKT phosphorylation, which promotes cell migration and invasion.

Conclusion

Our results indicated that vasculostatin-expressing OV therapy enhanced chemotherapy with bevacizumab for malignant glioma by suppressing bevacizumab-induced glioma invasion via the AKT signaling pathway. This may be a potential combination therapy for clinical use in patients with malignant

glioma.

Acknowledgments

We thank M. Arao and Y. Ukai for their technical assistance. We thank Nancy Schatken, BS, MT (ASCP), from Edanz Group (www.edanzediting.com/ac) for editing a draft of this manuscript.

References

1. Penas-Prado M, Gilbert MR. Molecularly targeted therapies for malignant gliomas: advances and challenges. *Expert Rev Anticancer Ther* **2007**;7(5):641-61 doi 10.1586/14737140.7.5.641.
2. Sim HW, Morgan ER, Mason WP. Contemporary management of high-grade gliomas. *CNS Oncol* **2017** doi 10.2217/cns-2017-0026.
3. Stupp R, Mason WP, van den Bent MJ, Weller M, Fisher B, Taphoorn MJ, *et al.* Radiotherapy plus concomitant and adjuvant temozolomide for glioblastoma. *N Engl J Med* **2005**;352(10):987-96 doi 10.1056/NEJMoa043330.
4. Vredenburgh JJ, Desjardins A, Herndon JE, 2nd, Dowell JM, Reardon DA, Quinn JA, *et al.* Phase II trial of bevacizumab and irinotecan in recurrent malignant glioma. *Clinical cancer research : an official journal of the American Association for Cancer Research* **2007**;13(4):1253-9 doi 10.1158/1078-0432.ccr-06-2309.
5. Chinot OL, Wick W, Mason W, Henriksson R, Saran F, Nishikawa R, *et al.* Bevacizumab plus radiotherapy-temozolomide for newly diagnosed glioblastoma. *N Engl J Med* **2014**;370(8):709-22 doi 10.1056/NEJMoa1308345.
6. Gilbert MR, Dignam JJ, Armstrong TS, Wefel JS, Blumenthal DT, Vogelbaum MA, *et al.* A randomized trial of bevacizumab for newly diagnosed glioblastoma. *N Engl J Med* **2014**;370(8):699-708 doi 10.1056/NEJMoa1308573.
7. Ishida J, Onishi M, Kurozumi K, Ichikawa T, Fujii K, Shimazu Y, *et al.* Integrin inhibitor suppresses bevacizumab-induced glioma invasion. *Transl Oncol* **2014**;7(2):292-302.e1 doi 10.1016/j.tranon.2014.02.016.
8. Piao Y, Liang J, Holmes L, Zurita AJ, Henry V, Heymach JV, *et al.* Glioblastoma resistance to anti-VEGF therapy is associated with myeloid cell infiltration, stem cell accumulation, and a mesenchymal phenotype. *Neuro-oncology* **2012**;14(11):1379-92 doi 10.1093/neuonc/nos158.
9. Kurozumi K, Hardcastle J, Thakur R, Shroll J, Nowicki M, Otsuki A, *et al.* Oncolytic HSV-1 infection of tumors induces angiogenesis and upregulates CYR61. *Molecular therapy : the journal of the American Society of Gene Therapy* **2008**;16(8):1382-91 doi 10.1038/mt.2008.112.
10. Eissa IR, Naoe Y, Bustos-Villalobos I, Ichinose T, Tanaka M, Zhiwen W, *et al.* Genomic Signature of the Natural Oncolytic Herpes Simplex Virus HF10 and Its Therapeutic Role in Preclinical and Clinical Trials. *Frontiers in oncology* **2017**;7:149 doi 10.3389/fonc.2017.00149.
11. Andtbacka RH, Kaufman HL, Collichio F, Amatruda T, Senzer N, Chesney J, *et*

- al.* Talimogene Laherparepvec Improves Durable Response Rate in Patients With Advanced Melanoma. *Journal of clinical oncology : official journal of the American Society of Clinical Oncology* **2015**;33(25):2780-8 doi 10.1200/jco.2014.58.3377.
12. Fujii K, Kurozumi K, Ichikawa T, Onishi M, Shimazu Y, Ishida J, *et al.* The integrin inhibitor cilengitide enhances the anti-glioma efficacy of vasculostatin-expressing oncolytic virus. *Cancer Gene Ther* **2013**;20(8):437-44 doi 10.1038/cgt.2013.38.
 13. Hardcastle J, Kurozumi K, Dmitrieva N, Sayers MP, Ahmad S, Waterman P, *et al.* Enhanced antitumor efficacy of vasculostatin (Vstat120) expressing oncolytic HSV-1. *Molecular therapy : the journal of the American Society of Gene Therapy* **2010**;18(2):285-94 doi 10.1038/mt.2009.232.
 14. Kambara H, Okano H, Chiocca EA, Saeki Y. An oncolytic HSV-1 mutant expressing ICP34.5 under control of a nestin promoter increases survival of animals even when symptomatic from a brain tumor. *Cancer research* **2005**;65(7):2832-9 doi 10.1158/0008-5472.can-04-3227.
 15. Oka T, Kurozumi K, Shimazu Y, Ichikawa T, Ishida J, Otani Y, *et al.* A super gene expression system enhances the anti-glioma effects of adenovirus-mediated REIC/Dkk-3 gene therapy. *Sci Rep* **2016**;6:33319 doi 10.1038/srep33319.
 16. Shimazu Y, Kurozumi K, Ichikawa T, Fujii K, Onishi M, Ishida J, *et al.* Integrin antagonist augments the therapeutic effect of adenovirus-mediated REIC/Dkk-3 gene therapy for malignant glioma. *Gene Ther* **2015**;22(2):146-54 doi 10.1038/gt.2014.100.
 17. Yoo JY, Haseley A, Bratasz A, Chiocca EA, Zhang J, Powell K, *et al.* Antitumor efficacy of 34.5ENVE: a transcriptionally retargeted and "Vstat120"-expressing oncolytic virus. *Molecular therapy : the journal of the American Society of Gene Therapy* **2012**;20(2):287-97 doi 10.1038/mt.2011.208.
 18. Kaur B, Brat DJ, Devi NS, Van Meir EG. Vasculostatin, a proteolytic fragment of brain angiogenesis inhibitor 1, is an antiangiogenic and antitumorigenic factor. *Oncogene* **2005**;24(22):3632-42 doi 10.1038/sj.onc.1208317.
 19. Kaur B, Cork SM, Sandberg EM, Devi NS, Zhang Z, Klenotic PA, *et al.* Vasculostatin inhibits intracranial glioma growth and negatively regulates in vivo angiogenesis through a CD36-dependent mechanism. *Cancer research* **2009**;69(3):1212-20 doi 10.1158/0008-5472.can-08-1166.
 20. Nishimori H, Shiratsuchi T, Urano T, Kimura Y, Kiyono K, Tatsumi K, *et al.* A novel brain-specific p53-target gene, BAI1, containing thrombospondin type 1

- repeats inhibits experimental angiogenesis. *Oncogene* **1997**;15(18):2145-50.
21. Wang W, Da R, Wang M, Wang T, Qi L, Jiang H, *et al.* Expression of brain-specific angiogenesis inhibitor 1 is inversely correlated with pathological grade, angiogenesis and peritumoral brain edema in human astrocytomas. *Oncol Lett* **2013**;5(5):1513-8 doi 10.3892/ol.2013.1250.
 22. Wakimoto H, Kesari S, Farrell CJ, Curry WT, Jr., Zaupa C, Aghi M, *et al.* Human glioblastoma-derived cancer stem cells: establishment of invasive glioma models and treatment with oncolytic herpes simplex virus vectors. *Cancer research* **2009**;69(8):3472-81 doi 10.1158/0008-5472.Can-08-3886.
 23. Wakimoto H, Mohapatra G, Kanai R, Curry WT, Jr., Yip S, Nitta M, *et al.* Maintenance of primary tumor phenotype and genotype in glioblastoma stem cells. *Neuro-oncology* **2012**;14(2):132-44 doi 10.1093/neuonc/nor195.
 24. Kaur B, Brat DJ, Calkins CC, Van Meir EG. Brain angiogenesis inhibitor 1 is differentially expressed in normal brain and glioblastoma independently of p53 expression. *Am J Pathol* **2003**;162(1):19-27 doi 10.1016/s0002-9440(10)63794-7.
 25. Terada K, Wakimoto H, Tyminski E, Chiocca EA, Saeki Y. Development of a rapid method to generate multiple oncolytic HSV vectors and their in vivo evaluation using syngeneic mouse tumor models. *Gene Ther* **2006**;13(8):705-14 doi 10.1038/sj.gt.3302717.
 26. Shimizu T, Ishida J, Kurozumi K, Ichikawa T, Otani Y, Oka T, *et al.* delta-Catenin Promotes Bevacizumab-Induced Glioma Invasion. *Molecular cancer therapeutics* **2019**;18(4):812-22 doi 10.1158/1535-7163.Mct-18-0138.
 27. Otani Y, Ichikawa T, Kurozumi K, Inoue S, Ishida J, Oka T, *et al.* Fibroblast growth factor 13 regulates glioma cell invasion and is important for bevacizumab-induced glioma invasion. *Oncogene* **2017** doi 10.1038/onc.2017.373.
 28. Young N, Pearl DK, Van Brocklyn JR. Sphingosine-1-phosphate regulates glioblastoma cell invasiveness through the urokinase plasminogen activator system and CCN1/Cyr61. *Molecular cancer research : MCR* **2009**;7(1):23-32 doi 10.1158/1541-7786.Mcr-08-0061.
 29. Kurozumi K, Hardcastle J, Thakur R, Yang M, Christoforidis G, Fulci G, *et al.* Effect of tumor microenvironment modulation on the efficacy of oncolytic virus therapy. *J Natl Cancer Inst* **2007**;99(23):1768-81 doi 10.1093/jnci/djm229.
 30. Tan G, Kasuya H, Sahin TT, Yamamura K, Wu Z, Koide Y, *et al.* Combination therapy of oncolytic herpes simplex virus HF10 and bevacizumab against

- experimental model of human breast carcinoma xenograft. *Int J Cancer* **2015**;136(7):1718-30 doi 10.1002/ijc.29163.
31. de Groot JF, Fuller G, Kumar AJ, Piao Y, Eterovic K, Ji Y, *et al.* Tumor invasion after treatment of glioblastoma with bevacizumab: radiographic and pathologic correlation in humans and mice. *Neuro-oncology* **2010**;12(3):233-42 doi 10.1093/neuonc/nop027.
 32. Jahangiri A, Nguyen A, Chandra A, Sidorov MK, Yagnik G, Rick J, *et al.* Cross-activating c-Met/beta1 integrin complex drives metastasis and invasive resistance in cancer. *Proc Natl Acad Sci U S A* **2017**;114(41):E8685-e94 doi 10.1073/pnas.1701821114.
 33. Kang X, Xiao X, Harata M, Bai Y, Nakazaki Y, Soda Y, *et al.* Antiangiogenic activity of BAI1 in vivo: implications for gene therapy of human glioblastomas. *Cancer Gene Ther* **2006**;13(4):385-92 doi 10.1038/sj.cgt.7700898.
 34. Fukushima Y, Oshika Y, Tsuchida T, Tokunaga T, Hatanaka H, Kijima H, *et al.* Brain-specific angiogenesis inhibitor 1 expression is inversely correlated with vascularity and distant metastasis of colorectal cancer. *Int J Oncol* **1998**;13(5):967-70.
 35. Hatanaka H, Oshika Y, Abe Y, Yoshida Y, Hashimoto T, Handa A, *et al.* Vascularization is decreased in pulmonary adenocarcinoma expressing brain-specific angiogenesis inhibitor 1 (BAI1). *Int J Mol Med* **2000**;5(2):181-3.
 36. Lee JH, Koh JT, Shin BA, Ahn KY, Roh JH, Kim YJ, *et al.* Comparative study of angiostatic and anti-invasive gene expressions as prognostic factors in gastric cancer. *Int J Oncol* **2001**;18(2):355-61.
 37. Aghi M, Rabkin SD, Martuza RL. Angiogenic response caused by oncolytic herpes simplex virus-induced reduced thrombospondin expression can be prevented by specific viral mutations or by administering a thrombospondin-derived peptide. *Cancer research* **2007**;67(2):440-4 doi 10.1158/0008-5472.can-06-3145.
 38. DeLay M, Jahangiri A, Carbonell WS, Hu YL, Tsao S, Tom MW, *et al.* Microarray analysis verifies two distinct phenotypes of glioblastomas resistant to antiangiogenic therapy. *Clinical cancer research : an official journal of the American Association for Cancer Research* **2012**;18(10):2930-42 doi 10.1158/1078-0432.ccr-11-2390.
 39. Haseley A, Boone S, Wojton J, Yu L, Yoo JY, Yu J, *et al.* Extracellular matrix protein CCN1 limits oncolytic efficacy in glioma. *Cancer research* **2012**;72(6):1353-62 doi 10.1158/0008-5472.can-11-2526.

40. Klenotic PA, Huang P, Palomo J, Kaur B, Van Meir EG, Vogelbaum MA, *et al.* Histidine-rich glycoprotein modulates the anti-angiogenic effects of vasculostatin. *Am J Pathol* **2010**;176(4):2039-50 doi 10.2353/ajpath.2010.090782.
41. Koh JT, Kook H, Kee HJ, Seo YW, Jeong BC, Lee JH, *et al.* Extracellular fragment of brain-specific angiogenesis inhibitor 1 suppresses endothelial cell proliferation by blocking alphavbeta5 integrin. *Exp Cell Res* **2004**;294(1):172-84 doi 10.1016/j.yexcr.2003.11.008.
42. Otani Y, Ishida J, Kurozumi K, Oka T, Shimizu T, Tomita Y, *et al.* PIK3R1Met326Ile germline mutation correlates with cysteine-rich protein 61 expression and poor prognosis in glioblastoma. *Sci Rep* **2017**;7(1):7391 doi 10.1038/s41598-017-07745-0.
43. Goodwin CR, Lal B, Zhou X, Ho S, Xia S, Taeger A, *et al.* Cyr61 mediates hepatocyte growth factor-dependent tumor cell growth, migration, and Akt activation. *Cancer research* **2010**;70(7):2932-41 doi 10.1158/0008-5472.Can-09-3570.
44. Han S, Bui NT, Ho MT, Kim YM, Cho M, Shin DB. Dexamethasone Inhibits TGF-beta1-Induced Cell Migration by Regulating the ERK and AKT Pathways in Human Colon Cancer Cells Via CYR61. *Cancer research and treatment : official journal of Korean Cancer Association* **2016**;48(3):1141-53 doi 10.4143/crt.2015.209.
45. Paw I, Carpenter RC, Watabe K, Debinski W, Lo HW. Mechanisms regulating glioma invasion. *Cancer Lett* **2015**;362(1):1-7 doi 10.1016/j.canlet.2015.03.015.
46. Ikeda K, Ichikawa T, Wakimoto H, Silver JS, Deisboeck TS, Finkelstein D, *et al.* Oncolytic virus therapy of multiple tumors in the brain requires suppression of innate and elicited antiviral responses. *Nat Med* **1999**;5(8):881-7 doi 10.1038/11320.
47. Libertini S, Iacuzzo I, Perruolo G, Scala S, Ierano C, Franco R, *et al.* Bevacizumab increases viral distribution in human anaplastic thyroid carcinoma xenografts and enhances the effects of E1A-defective adenovirus dl922-947. *Clinical cancer research : an official journal of the American Association for Cancer Research* **2008**;14(20):6505-14 doi 10.1158/1078-0432.Ccr-08-0200.
48. Walsh CT, Radeff-Huang J, Matteo R, Hsiao A, Subramaniam S, Stupack D, *et al.* Thrombin receptor and RhoA mediate cell proliferation through integrins and cysteine-rich protein 61. *FASEB journal : official publication of the Federation of American Societies for Experimental Biology* **2008**;22(11):4011-21 doi

- 10.1096/fj.08-113266.
49. Chinot OL, de La Motte Rouge T, Moore N, Zeaiter A, Das A, Phillips H, *et al.* AVAglio: Phase 3 trial of bevacizumab plus temozolomide and radiotherapy in newly diagnosed glioblastoma multiforme. *Adv Ther* **2011**;28(4):334-40 doi 10.1007/s12325-011-0007-3.
 50. Filley AC, Henriquez M, Dey M. Recurrent glioma clinical trial, CheckMate-143: the game is not over yet. *Oncotarget* **2017**;8(53):91779-94 doi 10.18632/oncotarget.21586.
 51. Currier MA, Eshun FK, Sholl A, Chernoguz A, Crawford K, Divanovic S, *et al.* VEGF blockade enables oncolytic cancer virotherapy in part by modulating intratumoral myeloid cells. *Molecular therapy : the journal of the American Society of Gene Therapy* **2013**;21(5):1014-23 doi 10.1038/mt.2013.39.

Figure 1. Cytotoxicity effect of RAMBO, bevacizumab, and their combination on glioma cell lines.

U87ΔEGFR, U251MG, U87MG, and MGG23 glioma cells were treated with saline or bevacizumab at a concentration of 10 μg/ml and infected with saline or RAMBO at a MOI of 0.1. (A) Representative images of U87ΔEGFR and MGG23 glioma cells undergoing cytotoxicity by RAMBO. (B) Cell viability was examined by WST-1 proliferation assay every 24 hours after infection. Data shown are the proportion of viable cells relative to those treated with saline as a control. Values are the mean ± SEM from five independent experiments. Statistical significance was calculated by analysis of variance with one-way ANOVA with Tukey's post hoc test. * p<0.001 compared between the indicated groups. CvR, control versus RAMBO; CvBR, control versus bevacizumab and RAMBO; BvR, bevacizumab versus RAMBO; BvBR, bevacizumab versus bevacizumab and RAMBO.

Figure 2. Inhibition of glioma cell migration.

Glioma cell lines were incubated with conditioned medium (CM) derived from glioma cells treated with RAMBO. Additionally, they were treated with the indicated concentration of bevacizumab. Giemsa staining was performed 24 hours after treatment. (A) Representative images from the scratch wound assay. (B) Glioma cells migrating into the scratch area were assayed. Data shown are the proportions of migrating cells against whole cells in the field relative to those treated with saline as a control. (C) Representative images from the two-chamber migration assay. (D) Migrating cells were counted 24 hours after treatment. Data shown are the migrating cells relative to those treated with saline as a control.

Values are the mean ± SEM from five independent experiments. Statistical significance was calculated by analysis of one-way ANOVA with Tukey's post hoc test. *p<0.05, **p<0.01 and ***p<0.001 compared between the indicated groups.

Figure 3. Inhibition of glioma cell invasion.

(A) Representative images from the two-chamber invasion assay. Glioma cell lines were incubated with conditioned medium (CM) derived from glioma cells treated with RAMBO or HSVQ. Additionally, they were treated with the indicated concentration of bevacizumab. (B) Invading cells were counted 24 hours after treatment. Data shown are the invading cells relative to those treated with saline as a control. (C) Representative images of matrigel invasion assay. Spheroids of MGG23 cells were implanted into a 96-well plate, followed by treatment with viruses and bevacizumab. Then matrigel was

added to each well. (D) The invading cells observed outside the core spheroid were assayed. Data shown are the proportions of invading distance against core diameter relative to those treated with saline as a control.

Values are the mean \pm SEM from five independent experiments. Statistical significance was calculated by analysis of one-way ANOVA with Tukey's post hoc test. * $p < 0.05$, ** $p < 0.01$ and *** $p < 0.001$ compared between the indicated groups.

Figure 4. Kaplan–Meier survival curves and histological analysis of mice implanted with intracranial U87 Δ EGFR glioma cells.

(A) Glioma cell-bearing animals were administered saline or bevacizumab intraperitoneally on the indicated days and intratumoral saline or viruses on day 7. (B) Athymic nude mice bearing intracranial U87 Δ EGFR gliomas were treated with 1.0×10^5 pfu HSVQ or RAMBO, and bevacizumab was administered intraperitoneally at 10 mg/kg. Statistical significance was calculated by the log-rank test. (C) Immunohistochemical staining of the tumors with anti-human leukocyte antigen monoclonal antibody. The untreated tumor shows the expansion of the tumor with well-defined borders. After treatment with bevacizumab, the tumor border became irregular with tumor invasion. (D) The invasiveness—was assessed by the distance between the tumor mass edge and invasive lesion. Values are the mean \pm SEM from five independent experiments. Statistical significance was calculated by analysis of one-way ANOVA with Tukey's post hoc test. * $p = 0.010$, and ** $p < 0.006$ compared between the indicated groups.

Figure 5. Kaplan–Meier survival curves and histological analysis of mice implanted with intracranial MGG23 glioma cells.

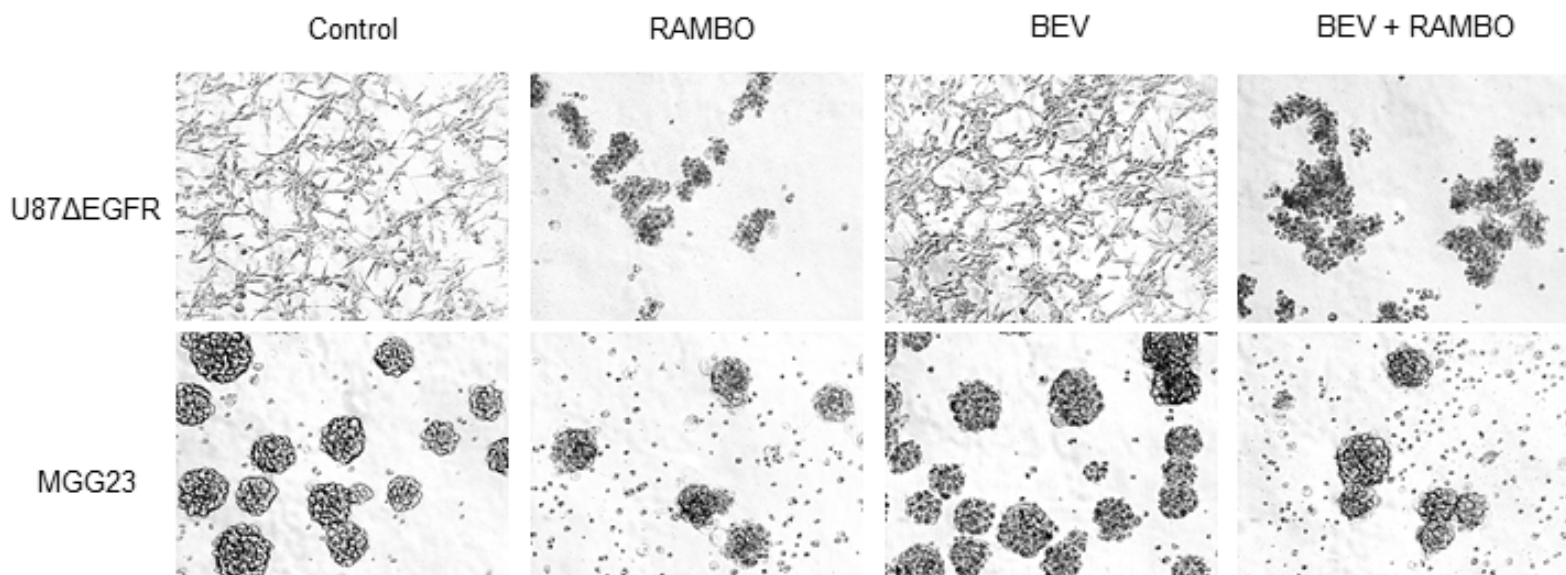
(A) Immunodeficient mice bearing intracranial MGG23 gliomas were treated with 1.0×10^5 pfu HSVQ or RAMBO, and bevacizumab was administered intraperitoneally at 10 mg/kg. Statistical significance was calculated by the log-rank test. (B) Immunohistochemical staining of the tumors with anti-human leukocyte antigen monoclonal antibody. MGG23 cells invaded to the ipsilateral cerebral cortex adjacent to the injection site and to the contralateral corpus callosum. Bevacizumab treatment increased invasion compared with saline or bevacizumab and RAMBO combination. (C) Values are the mean \pm SEM from five independent experiments. Statistical significance was calculated by analysis of one-way ANOVA with Tukey's post hoc test. * $p < 0.05$, ** $p < 0.01$ and *** $p < 0.001$ compared between the indicated groups.

Figure 6. Combination therapy with bevacizumab and RAMBO downregulated the AKT pathway compared with bevacizumab monotherapy.

Relative expression levels of CSK (A), SHC3 (B), PTK (C), CAV (D), SOS1 (E) and CCN1 (F) in the U87ΔEGFR mouse orthotopic model treated with bevacizumab. Only CCN1 expression was significantly reduced in the tumors treated with bevacizumab and RAMBO combination therapy compared with those treated with bevacizumab alone. Data shown are the mean ± SEM. Statistical significance was calculated by one-way analysis of variance followed by Scheffe's post hoc test, two-sided. * $p < 0.05$ compared between the indicated groups. (G) Immunoblot analysis of the levels of CCN1, p-AKT and AKT total protein in glioma cells. (H) Quantification of data from panel (A). Values are the mean ± SEM from five independent experiments. Statistical significance was calculated by analysis of one-way ANOVA with Tukey's post hoc test. * $p < 0.05$, ** $p < 0.01$ and *** $p < 0.001$ compared between the indicated groups.

Figure. 1

A.



B.

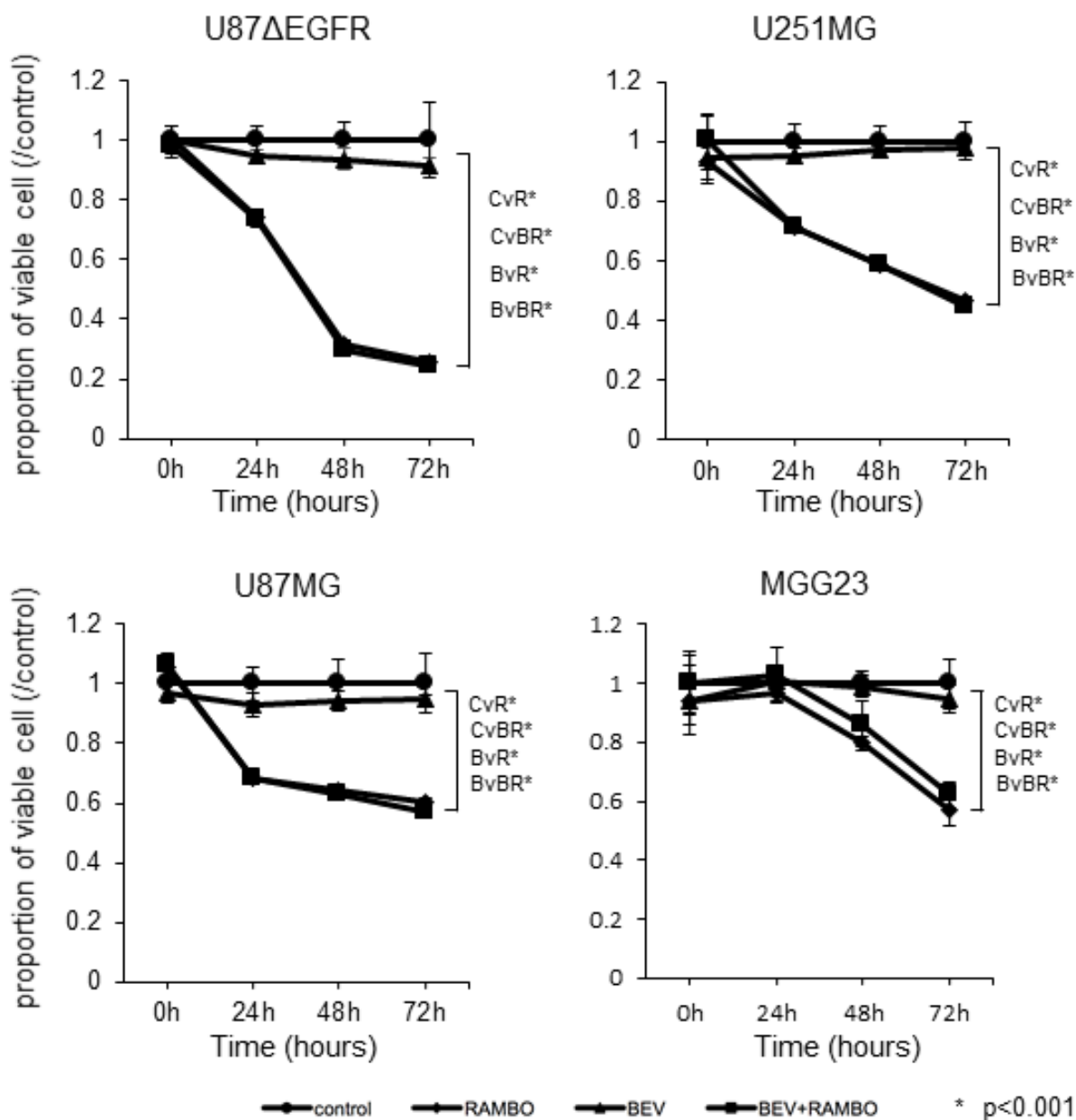


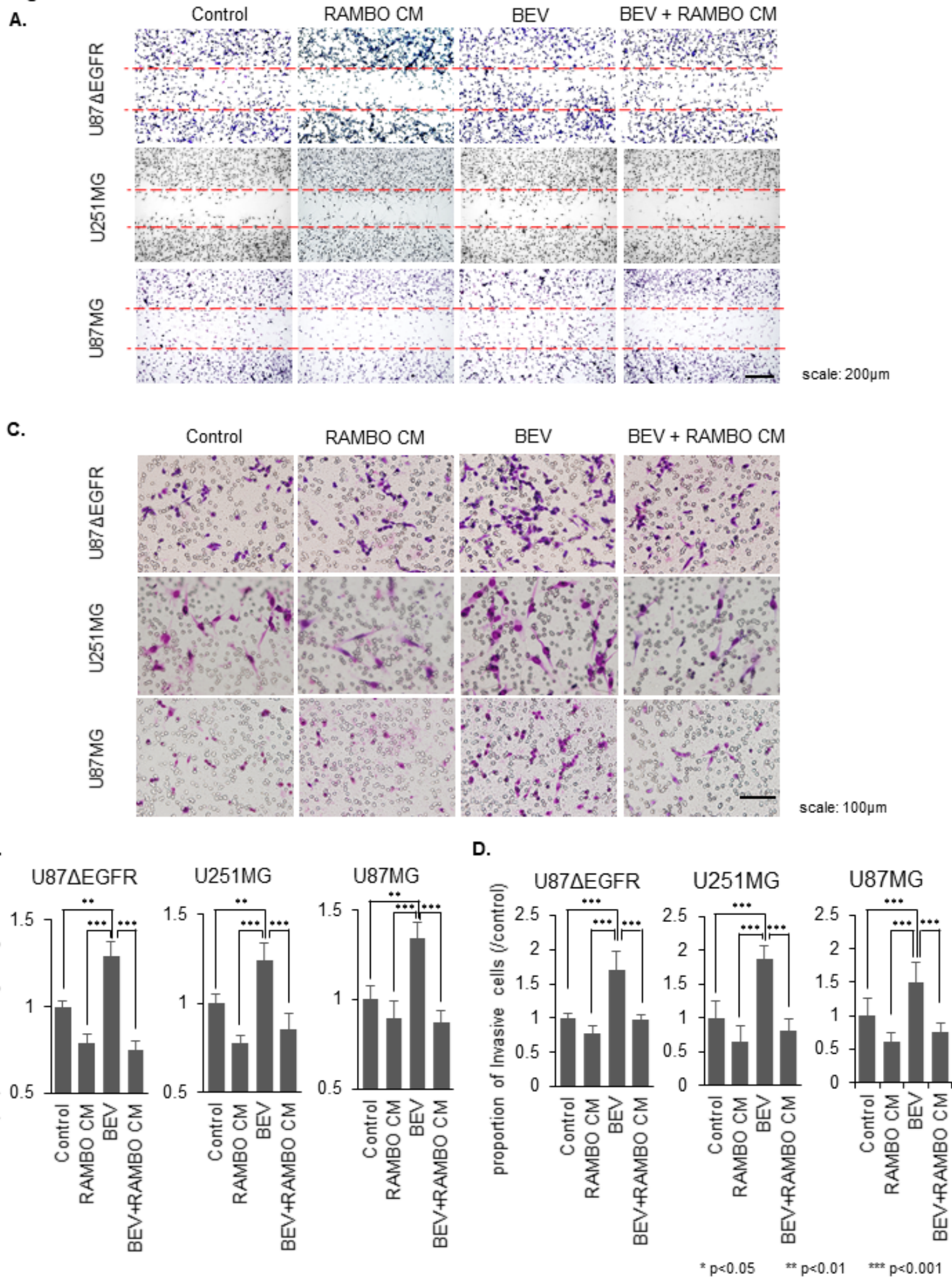
Figure. 2

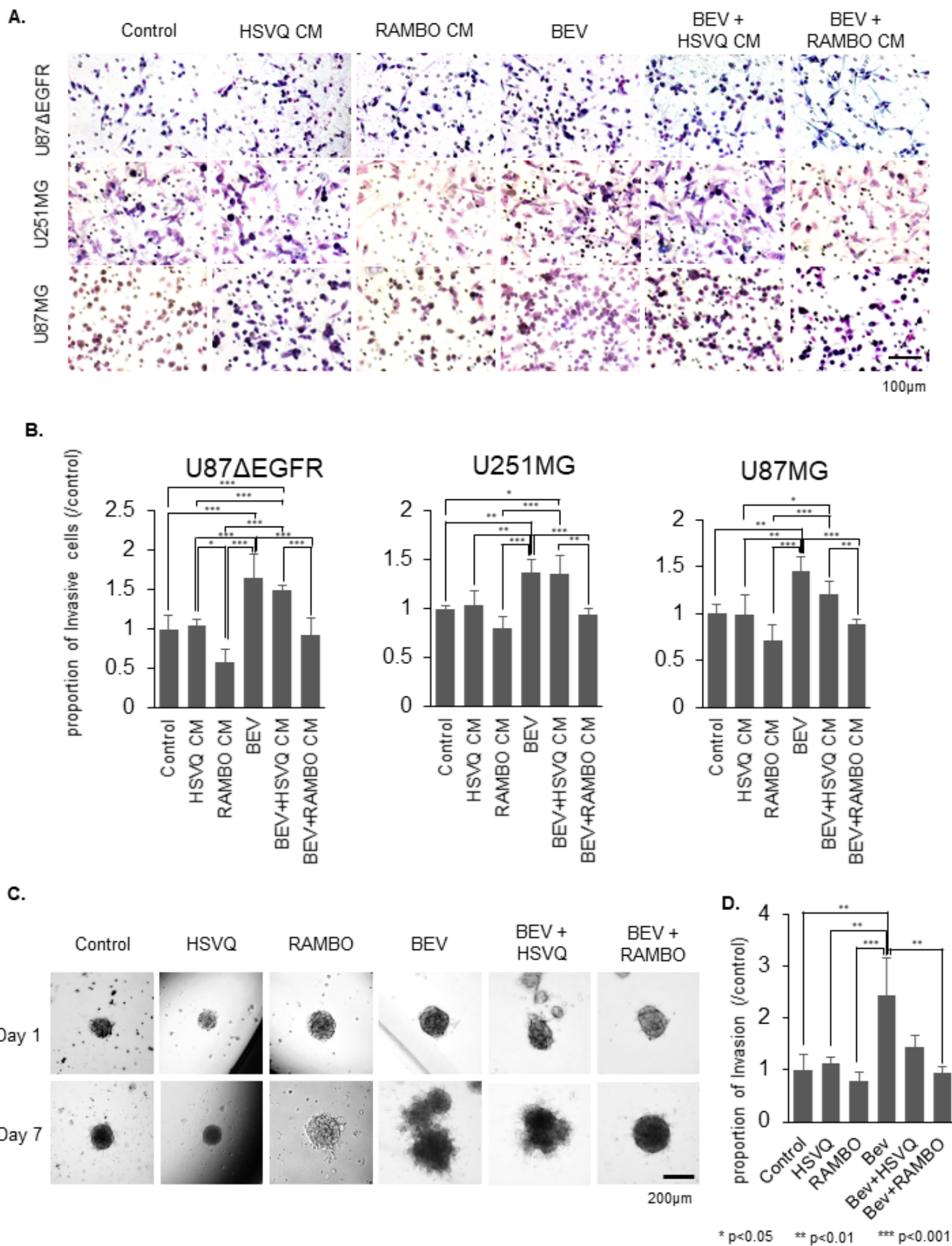
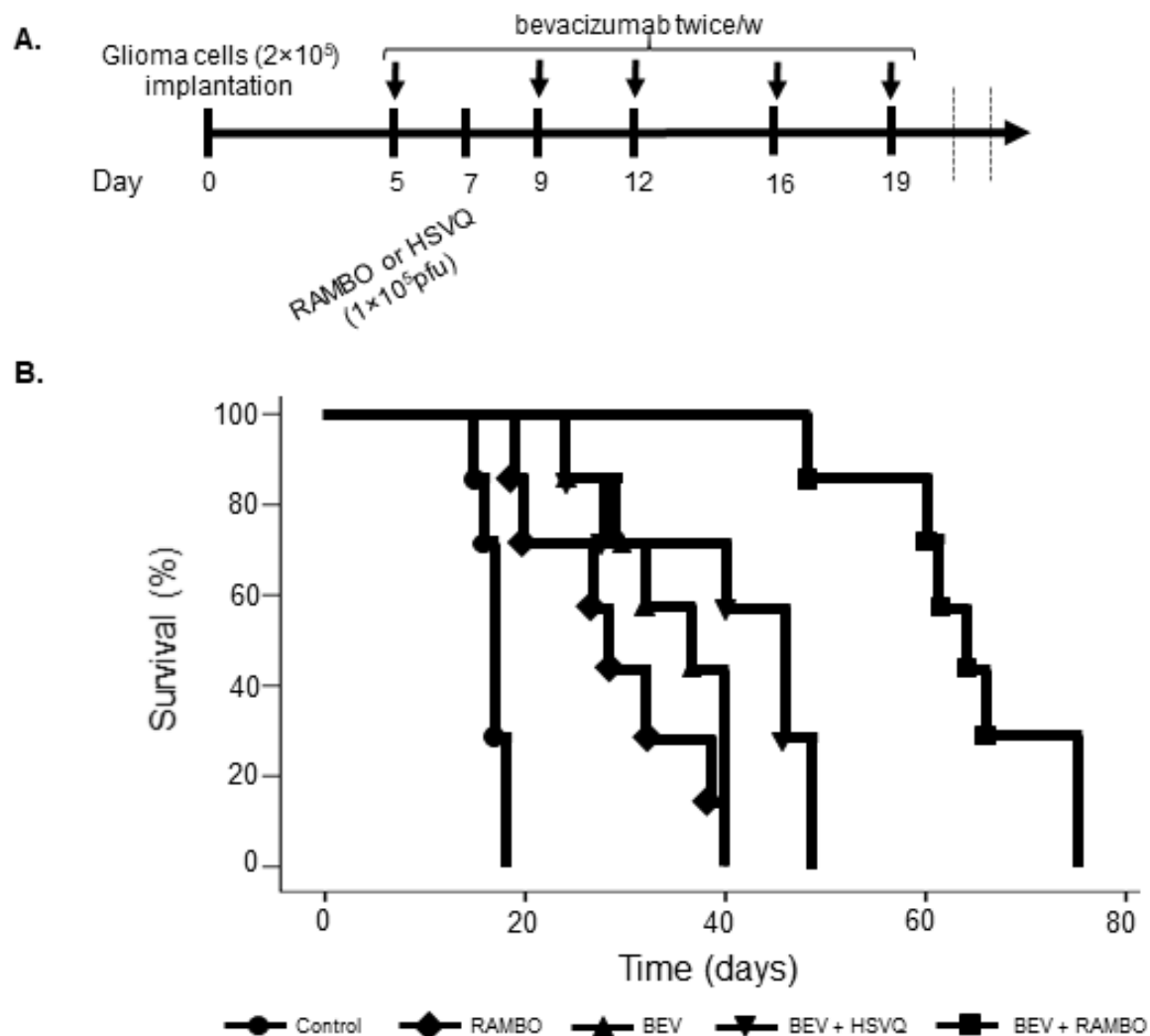
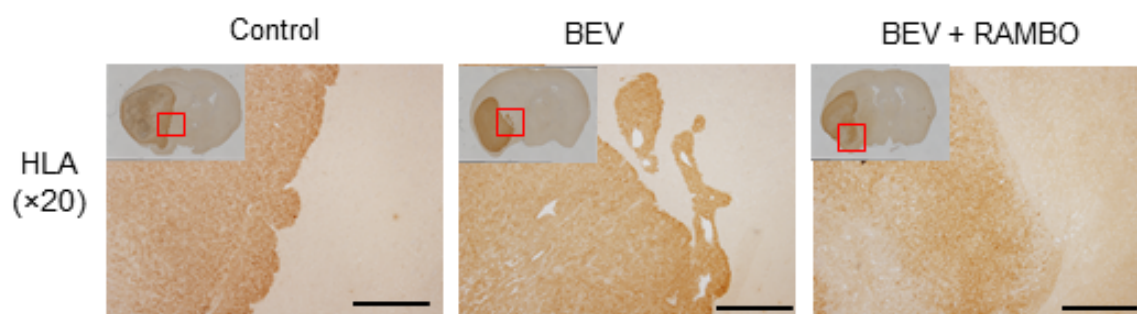
Figure 3

Figure.4

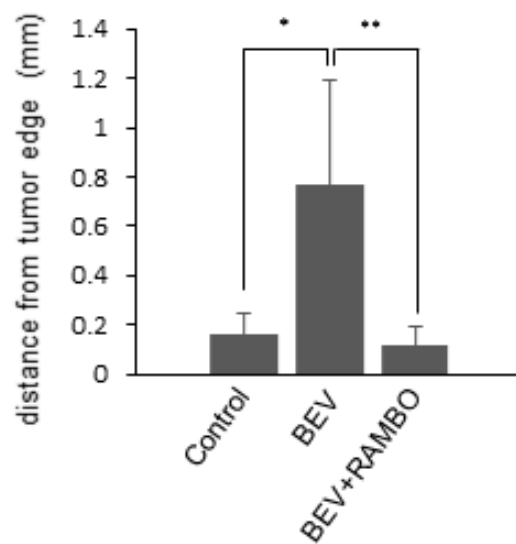


C.



bar 500 μ m

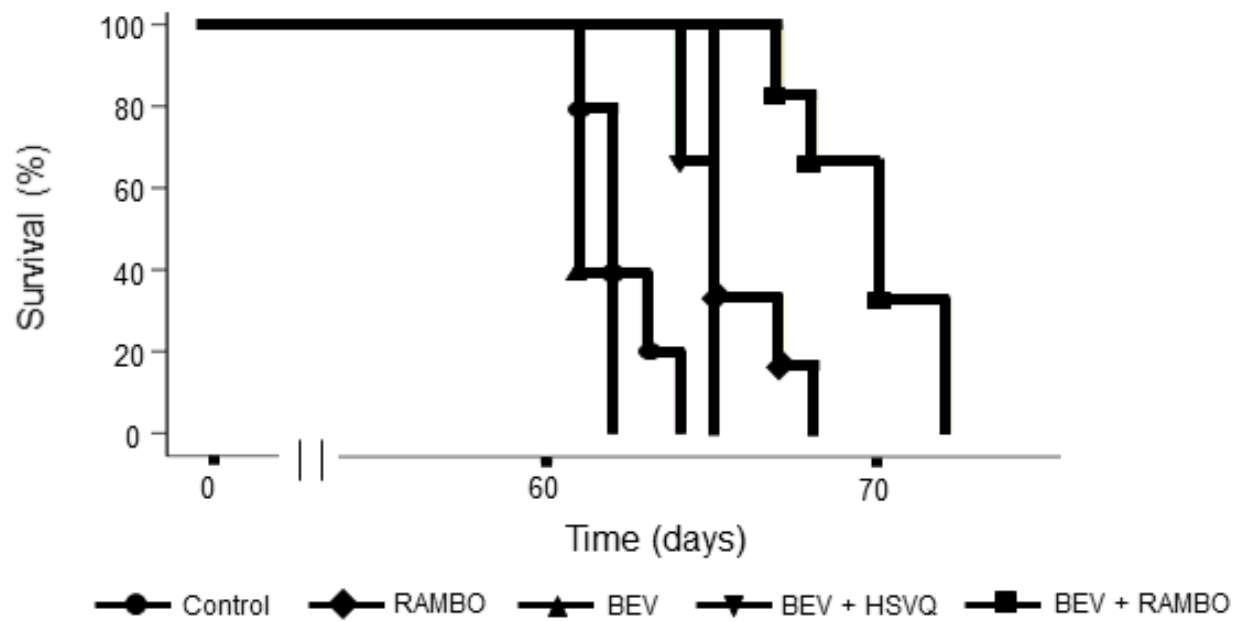
D.



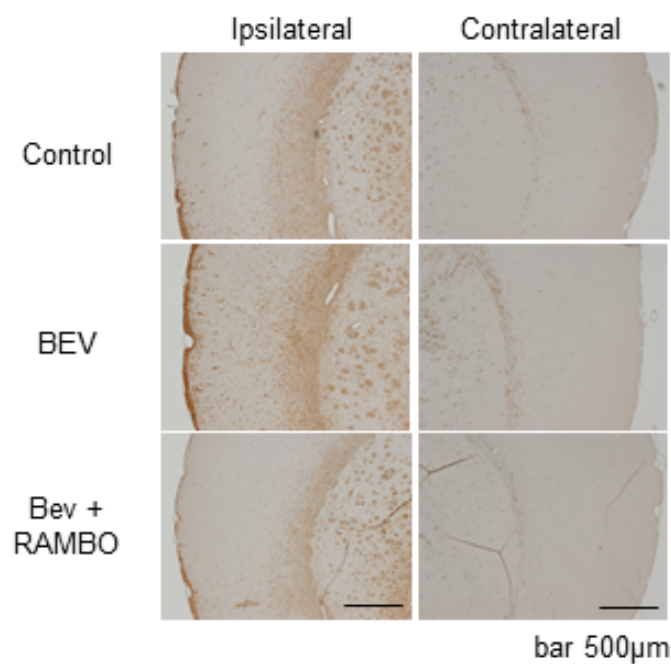
* $p=0.010$
** $p=0.006$

Figure. 5

A.



B.



C.

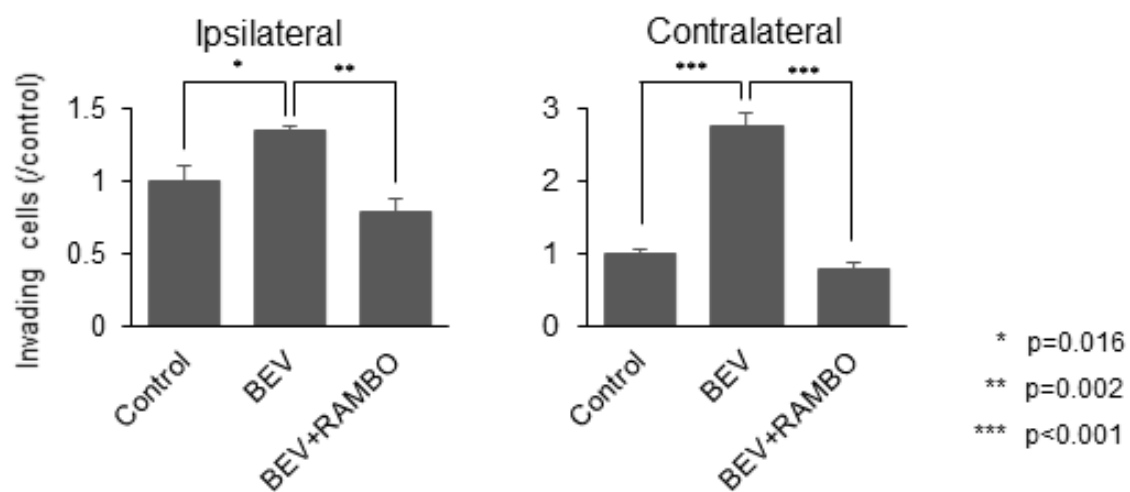


Figure 6